[4]W. K. Rhim, D. P. Burum, and D. D. Elleman, Phys. Rev. Lett. 37, 1764 (1976). L. N. Erovfeev and V. A. Shumm, Pis'ma Zh. Eksp. Teor. Fiz. 27, 161 (1978) [JETP Lett. 27, 149 (1978)].
[5]Yu. I. Ivanov, B. N. Provotorov, and E. B. Fel'dman, Pis'ma Zh. Eksp. Teor. Fiz. 27, 164 (1978) [JETP Lett. 27, 153 (1978)]; Zh. Eksp. Teor. Fiz. 75, 1847 (1978) [Sov. Phys. JETP 48, 930 (1978)].
[6]L. N. Erofeev, B. N. Provotorov, E. B. Fel'dman, and B. A. Shumm, Modern NMR and ESR Methods in Solid State Chemistry (Abstracts of 2nd All-Union Coordination Conference), 15, Chernogolovka, 1979.
[7]N. N. Bogolyubov and Yu. A. Mitropol'skiĭ, Asimptoticheskie metody v teorii nelineinykh kolebanii (Asymptotic Methods in the Theory of Nonlinear Oscillations), Nauka, 1974. Yu. A. Mitropol'skiĭ, Metod usredneniya v nelineĭnoĭ mekhanike (Averaging Method in Nonlinear Mechanics), Naukova dumka, 1971.
[8]F. S. Los', Ukr. Matem. Zh. 2, 3, 87 (1950).
[9]A. Abragam, Principles of Nuclear Magnetism, Oxford, 1960.
[10]T. Jeener, H. Eisendath, and R. Van Steenwinkel, Phys. Rev. A133, 478 (1964). L. L. Buishvili, N. P. Giorgadze, and M. D. Zviadadze, Zh. Eksp. Teor. Fiz. 73, 750 (1977) [Sov. Phys. JETP 46, 392 (1977)].
[11]J. L. Lowe and R. E. Norberg, Phys. Rev. 107, 46 (1957).
[12]M. Goldman, Spin Temperature and Nuclear Magnetic Resonance in Solids, Oxford, 1970. D. N. Zubarev, Neravnovesnaya statisticheskaya termodinamika (Nonequilibrium Statistical Thermodynamics, Nauka, 1971.
[13]L. N. Novikov and G. V. Skrotskiĭ, Usp. Fiz. Nauk 125, 449 (1978) [Sov. Phys. Usp. 21, 589 (1978)].

Translated by J. G. Adashko

Microstructure of a resistive layer on an aluminum surface

S. I. Dorozhkin and V. T. Dolgopolov

Institute of Solid State Physics, USSR Academy of Sciences
(Submitted 18 June 1979)
Zh. Eksp. Teor. Fiz. 77, 2443–2460 (December 1979)

The microstructure of the resistive layer formed on the surface of superconducting aluminum after switching off an external magnetic field $H_0 > H_c$ is investigated by using point junctions of size $d_0 \ll \xi_0$ (ξ_0 is the superconducting coherence length in aluminum. The macroscopic properties of the layer are close to the well-known properties of a two-dimensional mixed (TDM) state in type-*I* superconductors [Landau and Sharvin, JETP Lett. **10**, 121 (1969)]. It is found that, under various conditions, three types of structure exist in the layer, viz., stationary laminar, stationary island, and nonstationary island. The laminar structure is close to the model of the TDM state proposed by Gor'kov and Dorokhov [Sov. Phys. JETP **40**, 956 (1975)]. It is found that the structures move along the surface and that the dynamics of the structures is qualitatively the same as in the intermediate state [Gubankov and Margolin, JETP Lett. **29**, 673 (1979)]. On the basis of an analysis of the waveforms of the signals from the point junctions it is concluded that regions exist in which the order parameter varies from zero up to the superconducting value. The measured layer thickness $d \sim \xi_0$. The surface impedance differs from that corresponding to the pure superconducting state.

PACS numbers: 74.70.Gj, 73.25. + i

Among the resistive states of type-I superconductors, particular interest attaches to the two-dimensional mixed (TDM) state observed by I. Landau and Sharvin.[1] This state is produced on the inner surface of a hollow cylinder under the influence of a strong current flowing through it, when the ordinary intermediate-state structure is no longer present in the sample. An electric field is present in the TDM layer, and the current flowing through it produces a magnetic-field discontinuity $\Delta H \ll 2H_c$ across the layer. Such a layer was subsequently produced in the interior and on the outer surface of a hollow cylinder.[2] The presence of the TDM state causes paramagnetic effects in solid[3] and hollow[4] current-carrying cylinders.

The study of the microscopic structure of the TDM state is of great interest because the various employed theoretical models[5-8] predict different microscopic arrangements. A possible criterion of the proximity of a layer to the TDM state may be the relation between its characteristic dimensions and the superconducting coherence length ξ_0. Consequently the most convenient for structural investigations of the TDM state are superconductors with large ξ_0, particularly aluminum ($\xi_0 = 1.36 \times 10^{-4}$ cm, Ref. 9).

We have previously noted[10] that a layer with properties close to those of the TDM state can be produced on the surface of a type-I superconductor when the external magnetic field $H_0 > H_c$ is turned off. In fact, the field outside the sample drops rapidly to zero, whereas in the interior of the sample, owing to the eddy currents, it remains equal to H_0 for a sufficiently long time. It follows from the continuity of the tangential component that the magnetic field is equal to zero also on the sample surface parallel to $\mathbf{H}_0$. The region near the surface, where $H < H_c$, should become superconducting. The produced layer cannot trap in the sample the magnetic flux, which at that time is larger than critical. The change of the magnetic flux passing through the sample leads to the appearance of a solenoidal electric field in the layer. Thus, a rather thin resistive layer should exist on the surface of the sample.

 0038-5646/79/121180-10$02.40

Even in our first experiments[10,11] it was observed with the aid of point junctions that the layer consists of moving normal and superconducting regions. The present study is a continuation of the investigation of the characteristics of the layer. Results are obtained for the case of a magnetic field that is parallel to the sample surface with high degree of accuracy (0.05°). The dimensions and speed of the structure are measured much more accurately than in the preceding work,[10] the dynamics of the structure is investigated in detail, and the waveforms of the signals from the point junctions are analyzed. The point-junction investigations are supplemented by a study of the surface impedance of the layer at frequencies 10^6–10^7 Hz and by a reliable measurement of its thickness.

EXPERIMENTAL PROCEDURE

The measurements were made on single-crystal aluminum samples. To study the microstructure of the layer, point junctions whose conductivity depends on the state of the sample region under the junction were produced on the sample surface. The time dependence of the junction voltage following the turning-off of the external magnetic field was investigated experimentally. The layer thickness was measured in individual experiments by using a coil wound around the sample. Additional information of the state of the layer was obtained by measuring the surface impedance.

The samples were 1×1×2 cm parallelepipeds cut from a single ingot with resistivity ratio $\rho_{300K}/\rho_{4.2K}=2\times10^4$. The roughnesses on the sample surfaces were removed by grinding, followed by etching the case-hardened layer in a 10% solution of NaOH. Electrolytic polishing in 75% ethyl alcohol and 25% hydrochloric acid at a current density 0.2 A/cm² produced a mirror finish. The surface quality was monitored with an MII-4 microinterferometer. The degree of perfection of the surface depended on the polishing time.

In the experiments we investigated the state of one sample face parallel to the (110) plane of the crystal. The measurements were made on five samples. A microinterferogram of the surface of the best of these samples (No. 5, polishing time two hours) is shown in Fig. 1. Noticeable deviations of the surface from a plane were observed only near its edges. Samples 1–4 were polished for 15 minutes and had worse surfaces, which were wavy with an approximate wave period 100 μm and approximate height 0.1 μm.

To produce the point junctions, several silver strips (usually six) were sputtered on the investigated sample surface. Electric breakdown was produced at helium temperatures in the oxide layer on the sample. The breakdown produced a microjunction between the sample and the silver film. To ensure a breakdown at a definite point, an SiO film was sputtered beforehand on the surface (see Fig. 2). The junctions were produced in the surface regions not covered by the silicon oxide, and the dimensions of these regions determined the accuracy with which the positions of the junctions were known. The slots in the mask used for the silver sputtering were produced by the electric-spark method using a tungsten wire of 0.05 mm diameter. The leads were secured to the sample and to the films with conducting adhesive. To prevent changes in the microjunction parameters as a result of diffusion, the sample was kept at a temperature lower than 78 K during the entire time of its investigation.

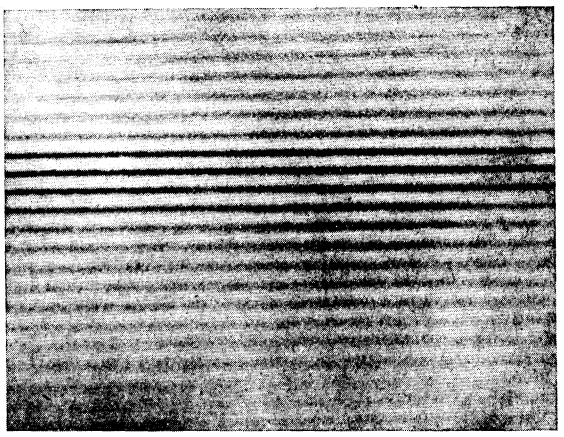

FIG. 1. Microinterferogram of the investigated surface in white light. Field of view 100×120 μm. Sample No. 5.

The microjunction resistance R_0 ranged from 10^{-2} to 1 Ω. The short-circuit dimensions, estimated by the formula proposed by Sharvin,[12] $R_0 \approx p_F/ne^2d_0^2$ (p_F is the Fermi momentum and n is the electron density), yields values $d_0 \approx 3\times10^{-6}$–$3\times10^{-5}$ cm, i.e., $d_0 \ll \xi_0$ in our case. A typical current-voltage characteristic of the junction is shown in Fig. 3. It is seen from the figure that if the current through the junction is fixed, then the state of the region of the sample under the junction can be determined from the voltage across the junction.

The voltage was measured by the four-point method. The current through the junction was usually several milliamperes. An increase of the current by as much as five times, up to the sensitivity limit of the apparatus, did not change the results. The voltage from the junction was fed to an amplifier having a bandwidth 20 Hz–1 MHz and an intrinsic noise level ~10^{-5} V, and then fed to one of the channels of a two-beam memory oscilliscope S8-11 (Fig. 4). It was possible to register simultaneously the signals from two junctions (Fig. 4 shows the circuit for recording the signal from only one

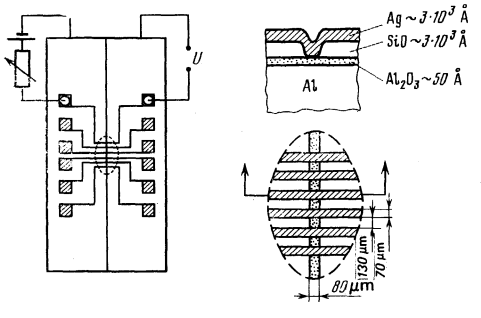

FIG. 2. Arrangement of point junctions on the investigated surface of the sample. The region in the dashed ellipse is shown magnified on the right.

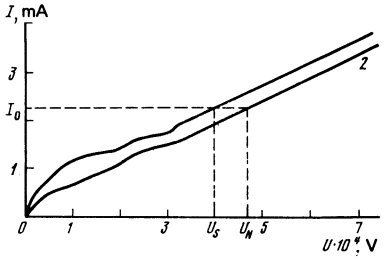

FIG. 3. Typical current-voltage characteristics of microjunction: 1—aluminum sample in the superconducting state, $H_0 = 0$; 2—sample in normal states, $H_0 = H_c$; $T = 0.4$ K. A current $I = I_0$ was made to flow through the junction in the experiments. When the region under the junction changes from the superconducting to the normal state the junction voltage changes from U_S to U_N.

junction). The oscilloscope sweep was started by a signal synchronized with the turning-off of the external field.

To measure the impedance, a flat coil of 20 turns of copper wire was placed on the surface. The coil was connected either to one of the arms of a twin-T bridge[13] operating at 15 MHz, or to the tank circuit of an RF oscillator. The bridge-unbalance signal was amplified by broadband amplifiers U3-7A and U3-33, detected, and fed to one of the oscilloscope channels, where it was recorded as a function of the time. The detector time constant was 10^{-4} sec. The sensitivity of the bridge circuit was approximately 4% of the difference between the impedances of the normal and superconducting states.

A higher measurement accuracy (about 0.5%) was obtained with the circuit shown in Fig. 4. Signals of frequency f from the measuring generator G and of frequency $f_0 \approx 1.5$ MHz from a reference generator G_0 were fed to the mixer mix. The frequency mixing produced a difference frequency whose period was measured in F571 electronic counting frequency meter. The measurement time could be either one or ten periods of the difference frequency (usually $\sim 1.2\times10^{-3}$ and 12×10^{-3} sec, respectively). The frequency meter was started by a signal from the time delay block TD. The instant of measurement of the impedance was selected by adjusting the delay time, which could be varied smoothly in the range 1–200 msec. At the instant when the counting stopped, the frequency meter generated a pulse fed to the second channel of the oscilloscope. This made it possible to measure the dependence of the surface impedance on the time.

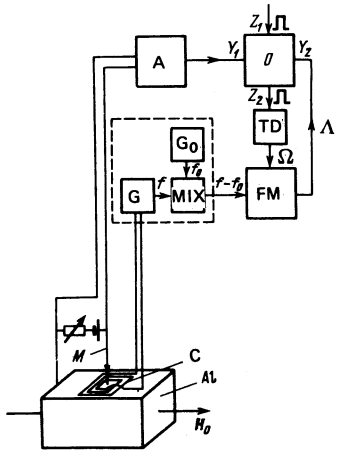

FIG. 4. Circuit used to measure the signal from the microjunction and the imaginary component of the surface impedance: Al—aluminum sample, C—flat coil, M—equivalent circuit of microjunction, A—U2-6 amplifier operating in the broadband regime, O—two-beam memory oscilloscope S8-11 (Y_1 and Y_2—its input channels Z_1—external triggering input, Z_2—input of signal synchronized with the instant of triggering of the oscilloscope sweep), G—measuring generator, G_0—reference generator, MIX—mixer (G, G_0, and MIX are standard blocks of the high-frequency inductance and capacitance meter E7-5A), FM—electronic counting frequency meter F571, TD—time-delay block, Ω—synchronizing, Λ—pulse that stops the frequency-meter reading.

In individual experiments we investigated the time dependence of the magnetic flux in the sample. For this purpose, a coil of 100 turns of 0.05 mm copper wire was wound around the perimeter of the sample. The slow variation of the flux through the coil (the time is of the order of 1 sec) was registered with an F18 microwebermeter and plotted with an x-y recorder. This determined the time during which the magnetic flux in the sample drops to its critical value $\Phi_c = H_c S$ (S is the sample cross-section area). In all the experiments this time exceeded 1 sec. The state of the surface layer was investigated during the first 100 msec after its formation. In the measurements of the thickness of the produced layer and of the average solenoidal electric field in the layer, the coil signal, which was proportional to the rate of change of the magnetic flux, was amplified and fed to the memory oscilloscope.

The magnetic field was produced by a Helmholtz coil mounted on the outside of the dewars. The maximun field was $H_0 = 360$ Oe, corresponding to supercriticality $H_0/H_c \approx 4$ at $T = 0.4$ K. Supercriticalities $H_0/H_c > 4$ were obtained at higher temperatures. The relative change of the field over the length of the sample was estimated to be less than 10^{-4}. The coil could be rotated in the horizontal plane through 360° (the sample was placed in the cryostat in such a way that the investigated surface was horizontal) and inclined in the vertical plane by an angle of approximately 4°. The field was turned off by mechanically opening the coil-supply circuit. Since the coil spool was made of copper, the magnetic-field fall-off time was determined by the damping of the eddy currents in the core. It amounted to ≈30 msec. The earth's magnetic field was cancelled out to within approximately 0.05 Oe with the aid of two compensating Helmholtz coils.

A temperature 0.4–1.2 K was obtained by pumping off He^3 vapor and was measured with a carbon resistance thermometer. By regulating the pump-off rate with a valve, it was possible to stabilize the temperature to within less than 5 mK. The sample was placed directly in the liquid He^3.

EXPERIMENTAL RESULTS

We report here the results of the investigation of the microstructure in the dynamics of the layer, as well as

the results of the measurements of its thickness and of its surface impedance.

1. As shown earlier,[10,11] the layer produced after the magnetic field is turned off is always inhomogeneous. It contains moving regions of the normal phase. At the instant of layer formation, the voltage on the microjunction changes within a time $\lesssim 10^{-5}$ sec from a value U_N to U_S (see Fig. 3). The passage of the normal regions under the contact causes the signal from the contact to consist of a number of pulses with a voltage that alternates between U_S and U_N (see Fig. 5).

The voltage on the junction following the layer formation was measured with a digital voltmeter. At the lowest concentration of the normal regions in the layer (less than 1%) this voltage, averaged over the measurement time (20 msec), agreed within $0.02(U_N - U_S)$ with the voltage U_S produced when the entire sample was superconducting.

The junction voltage pulses were trapezoidal (see Fig. 5). It must be specially noted that the waveform of the pulses is not governed by instrumental effects. The presence of gently sloping pulse fronts means a real existence of transition regions whose passage under the junction causes the junction voltage to vary between the values corresponding to the different states. We shall henceforth designate the time intervals corresponding to the trapezoid base by τ_N or $\bar{\tau}_N (\tau_N > \bar{\tau}_N)$ while the interval between neighboring pulses will be designated τ_S.

By rotating the magnetic field in the plane of the investigated surface it is possible to vary the locations of the normal regions and their direction of motion in such a way that the signals from two junctions are correlated at definite positions of the magnetic field (Fig. 6). Observation of correlated signals from different junctions makes it possible to determine the direction and velocity V of the motion of the normal and superconducting regions, while the parameters of the corresponding pulses determine the dimensions of these regions: $a_N = V\tau_N$ and $a_S = V\tau_S$. The dimension of the transition region $b_N = V(\tau_N - \bar{\tau}_N)/2$.

The layer produced after turning off a magnetic field

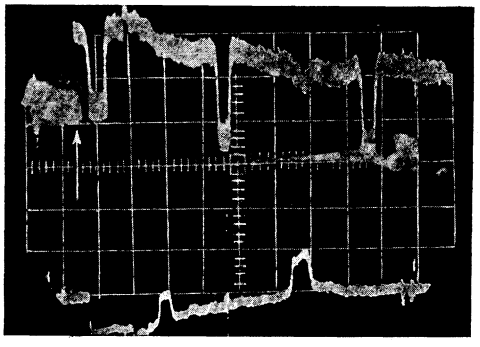

FIG. 5. Photograph from oscilloscope screen. Simultaneous record of signals from two junctions. The instant of layer formation is marked by the arrow. Angle of inclination of magnetic field to the sample surface $\theta = 1.9°$; $H_0/H_c = 2$, $T = 0.4$ K. Sample No. 1.

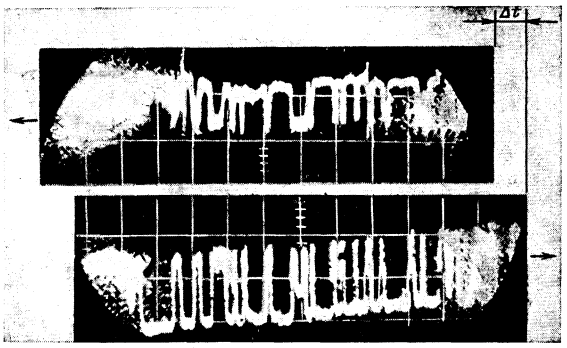

FIG. 6. Photograph from oscilloscope screen. For convenience in observation, the photograph is cut and the two halves are shifted along the t axis until the signals from the two junctions coincide at $\Delta t = 2$ msec; $\theta = 0.7°$, $T = 1.1$ K, $H_0/H_c = 10$. Horizontal scale—2 msec/div. Sample No. 3.

that is inclined relative to the surface (at an angle $0.2° \lesssim \theta < 3°$) and has low supercriticality $1 < H_0/H_c < 4$ consists of moving normal and superconducting strips elongated approximately in the direction of the projection $\mathbf{H}_\parallel$ of the magnetic field on the plane of the surface.[10] Rotation of the magnetic field in the plane of the surface through an angle φ rotates the structure through the same angle. This conclusion was based on the fact that the time difference Δt between the corresponding pulses from two junctions turned out to be linear function of the angle φ at small values of this angle. The angle φ was measured from the position at which the pulses from the junctions were in synchronism, i.e., $\Delta t(\varphi = 0) = 0$. In this position, the magnetic field is directed along the line joining the contacts. The accuracy with which the direction from contact to contact is known is usually 10°. The quantity $l \sin\varphi/\Delta t \approx l\varphi/\Delta t$ ($\mathbf{l}$ is a vector directed from junction 1 to junction 2 and $\Delta t = t_2 - t_1$, where t_i is the instant of time at which the particular region passes under the junction i) is equal to the velocity V of the strip in a direction perpendicular to the strip.

The strip length exceeded 1 mm. The quantity $a_N = V\tau_N$ determines the total width of the strips, including the normal region proper as well as the transitions reions. The dependence of a_N and b_N on the magnetic-field component normal to the sample surface, $H_\perp = (\mathbf{H}_0 \cdot \mathbf{N}) = H_0 \sin\theta$ ($\mathbf{N}$ is a unit vector normal to the surface) is shown in Fig. 7. It is seen from the figure that

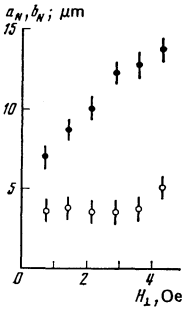

FIG. 7. Dependences of the widths of the normal-phase strips a_N (●) and of the widths of transition regions b_N (●) on the inclination of the magnetic field. Laminar structures; $H_0 = 160$ Oe, $T = 0.4$ K. Sample No. 2.

a_N increases approximately linearly with H_N, whereas $b_N \approx 3.5\times10^{-4}$ cm $= 2.5\xi_0$ does not depend on $H_\perp$ at our accuracy. The dimensions of the superconducting regions, $a_S \approx 2\times10^{-2}$ cm, depend little on $H_\perp$.

The dynamics of this laminar structure turned out to be quite complicated, and the results obtained with different samples were different. A variation was observed in the dependence of the sign of the velocity $V = l\sin\varphi/\Delta t$ on the magnetic-field direction. In samples 1 and 3, the sign of the velocity varied in accordance with the sign of the product $(\mathbf{H}_0\cdot\mathbf{N})(\mathbf{H}_0\cdot\mathbf{N})$ ($\mathbf{n}$ is a vector normal to the strips and lies in the plane of the surface), while in sample 2 it varied with the sign of $\eta\cdot\mathbf{H}_0\times\mathbf{N}$. In particular, in measurements on samples 1 and 3, in contrast to sample 2, the direction of motion did not change when the direction of the magnetic field was reversed. The velocity depends on the time differently for different samples and can change noticeably even when the direction of the magnetic field is changed (see Fig. 8). The results presented pertain to measurements made under conditions when the dependence of the velocity on the time was negligible.

A property common to all samples was the appreciable increase of the velocity with decreasing angle of inclination of the magnetic field (Fig. 9).

In an inclined magnetic field ($0.2° \lesssim \theta < 3°$) at high supercriticality $H_0/H_c \gtrsim 4$ the laminar structure gives way to an island structure[11] consisting apparently of closed normal regions. The structure moves approximately along the projection $\mathbf{H}_\parallel$ of the magnetic field on the surface plane. A correlation between the signal is present only in a narrow interval of the angle φ (2–5°) about a certain position. This position corresponds, with accuracy 3–4°, to a direction of a low supercriticality magnetic field such that the pulses from these two junctions are synchronized ($\varphi = 0$). The direction of motion does not depend on the sign of the field $\mathbf{H}_0$ and is reversed when the sign of the inclination angle θ of the field to the plane of the surface is reversed. The dependence of the velocity on the inclination angle is well described by the relation $V \sim 1/\theta$.[11] At a temperature 1.1 K, the dimensions of the normal regions lie in the range $a_N = (3–15)\times10^{-3}$ cm, while those of the transition regions are $b_N = (1.2–2.5)\times10^{3}$ cm.

The maximum supercriticality at which it was possible to observe the effects described above was ≈ 12. At $H_0/H_c > 12$ a stable superconducting layer is produced on the sample surface approximately 1 sec after the magnetic field is turned off.

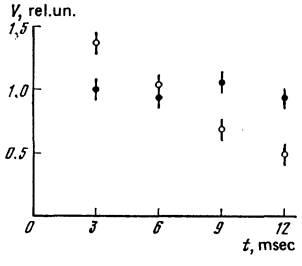

FIG. 8. Dependence of the velocity of the laminar structure on the time for sample No. 1; $T = 0.4$ K, $H_0/H_c = 2$. The points ● and ○ correspond to opposite directions of the field $\mathbf{H}_0$.

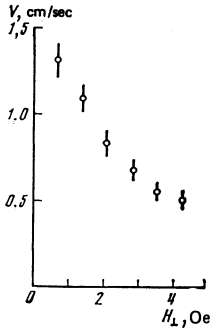

FIG. 9. Dependence of the velocity of the laminar structure on the inclination of the magnetic field: $H_0 = 160$ Oe, $T = 0.4$ K. Sample No. 2.

In a magnetic field parallel to the surface (accurate to ±0.05°) there is no correlation between signals from different junctions. This circumstance makes it impossible to determine directly the linear dimensions of the normal and superconducting regions. However, the signal-waveform singularities observed under these conditions do make it possible to identify the processes that occur on the surface.

When a field parallel to the surface is turned off, the pulses corresponding to the regions of the normal phase are spaced very irregularly. The pulse duration in a parallel field ($\sim 5\times10^{-5}$ sec) is smaller by approximately one order of magnitude than the corresponding value for the laminar structure at the minimal inclination angle at which correlation still exists.

The pulses are frequently asymmetrical with greatly differing edge durations. Frequently the leading front is the shorter (see Fig. 10). The heights of some pulses are noticeably smaller (by a factor 1.5–2) than $U_N - U_S$. Series of several pulses are observed in individual measurements, with a pulse off-duty cycle ~0.5 (see Fig. 11).

Long-duration regularly reproducible series were observed in sample No. 3 in a parallel field of large supercriticality. The total duration of the series reached 1000 msec, and the number of pulses in them reached 500 (see Fig. 12). The series were observed at definite

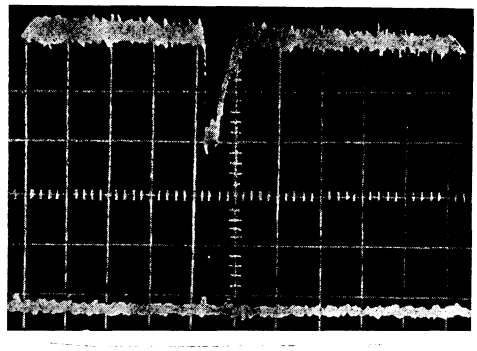

FIG. 10. Photograph from oscilloscope screen. The asymmetrical waveform of the pulse is clearly seen. $\theta = 0°$, $T = 1.1$ K, $H_0/H_c = 10$. Sample No. 1. Horizontal scale 100 μsec/div.

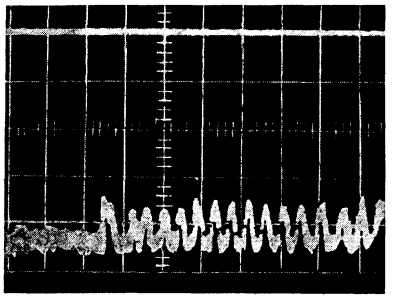

FIG. 11. Photograph from oscilloscope screen; $\theta = 0°$, $T = 1.1$ K, $H_0/H_c = 10$. Sample No. 5. Horizontal scale 100 μsec/div.

durations of the magnetic field in the plane of the surface and appeared 20–30 msec after the formation of the layer. A slight rotation of the field, through an angle $\varphi \approx 1°$, away from this direction caused the series to vanish. It is quite probable that these series stem from the normal regions produced on the edge of the sample.

2. The first measurement of the layer thicknesses was reported in Ref. 10. At the instant of layer formation, a voltage spike is produced by the coil wound on the sample. The abrupt change of the voltage is due to the forcing out of the magnetic flux from the region occupied by the layer. The thickness determined from the size of the spike turned out to be of the order of ξ_0. Such a measurement, however, could yield an incorrect result if an appreciable part of the magnetic flux is forced out of the layer into the interior of the sample.[14] To check on the validity of the foregoing estimate, we measured the voltage in a cycle in which the magnetic field was turned off and on. The magnetic field was parallel to the surface. Under these conditions, the concentration of the normal phase in the layer (see below) is minimal and does not exceed 5%. The time from the instant of formation of the layer to its annihilation was approximately 40 msec. At the instant of the annihilation of the layer, a voltage spike is likewise observed (Fig. 13) against the background of the signal due to the change of the magnetic flux through the gap between the sample and the coil. The flux that enters the sample is $\Delta\Phi \approx H_c P \xi_0$, where P is the perimeter of the sample cross section perpendicular to the magnetic field. The inaccuracy in the determination of the spike area, due to the presence of the large background, as

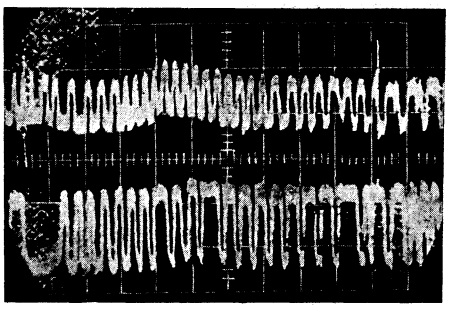

FIG. 12. Photograph from oscilloscope screen. Simultaneous record of signals from two junctions. $\theta = 0°$, $T = 1.1$ K, $H_0/H_c = 10$. Sample No. 3. Horizontal scale 1 msec/div.

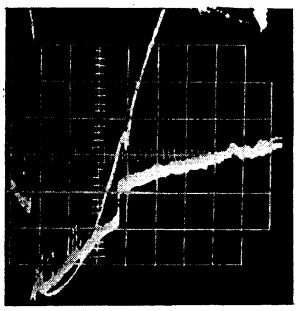

FIG. 13. Photograph from oscilloscope screen. Simultaneous record of signals from coil wound around the sample (upper curve) and from point junction (lower curve). $T = 0.65$ K, $H_0/H_c = 2$. Sample No. 1. Horizontal scale 10 msec/div, vertical scale 70 μV/div.

well as the inability to monitor the state of the entire sample surface, causes these measurements to yield only an estimate of the layer thickness, $d = (1-5)\xi_0$ at $T = 0.4$ K.

From the voltage induced in the coil it is also possible to determine the average electric field intensity E_j in the layer. For this purpose it suffices to measure the voltage at instant when the signal due to the change of the magnetic field in the gap between the sample and the coil has become negligibly small. It turns out that at a given field H_0 the value of E_j is independent of the angle θ between the magnetic field and the investigated sample surface ($|\theta| < 3°$) and varies only little, by approximately 20%, when the temperature is lowered below T_c. Consequently E_j is determined mainly by the damping of the eddy currents in the normal part of the sample. In the times during which the measurements were made the electric field was $E_j = (3 \pm 2) \times 10^{-7}$ V/cm (the uncertainty includes also the error due to the time variation of E_j) at $H_0 = 180$ Oe.

3. To obtain information on the state of the surface as a whole, measurements were made of the surface impedance. These measurements make it possible to obtain the concentration X_N of the normal phase on the surface, if the thickness of the investigated layer greatly exceeds the skin layer in the normal state and the latter, in turn, exceeds greatly the depth of penetration of the field into the semiconductor. In this case

$$X_N = (Z_x - Z_s)/(Z_N - Z_s),$$

where Z is the projection of the surface impedance on the arbitrary direction in the complex plane. The thickness of the skin layer and the normal aluminum at the frequency 1 MHz is of the order of the thickness of the investigated superconducting layer. To estimate the ensuing errors, the impedance was measured at frequencies 1.5 and 15 MHz. The impedance was measured during the first 20 msec following the layer formation, and under conditions when its time dependence could be neglected. Figure 14 shows plots of

$$\frac{U_x - U_s}{U_N - U_s}, \quad \frac{f_s - f_x}{f_s - f_N},$$

which are respectively the relative change of the bridge-unbalance signal and the relative change of the generator frequency, against the inclination of the mag-

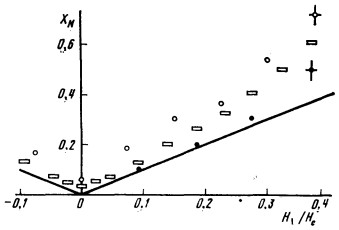

FIG. 14. Concentration X_N of normal phase in the layer as a function of the inclination of the magnetic field, determined by three different methods: ○—average relative duration of process corresponding to the normal phase, ●—measurements of the impedance of 15 MHz, □—measurements of the imaginary parts of the impedance at 1.5 MHz; straight line—plot corresponding to the intermediate state $X_N = H_\perp/H_c$, $T = 1.1$ K, $H_0/H_c = 10$. Sample No. 4.

netic field to the sample surface. The same figure shows the average relative duration of the pulses corresponding to the normal phase.

The most significant feature of these results is the difference between the surface impedance of the layer in a field parallel to the surface and the sample impedance in the superconducting state. As seen from the figures, this difference can be attributed to the presence of normal regions in the layer. The dependence of $X_N = (f_S - f_X)/(f_S - f_N)$ on the supercriticality, for a field H_0 parallel to the surface, is shown in Fig. 15. At our accuracy, the plot is a straight line passing through the origin. We varied the supercriticality by varying the magnetic field H_0 at constant temperature as well as by varying the temperature.

DISCUSSION OF RESULTS

The layer produced on the sample surface after turning off the magnetic field is in the resistive state. Two kinds of resistive state are possible in type-I superconductors, an intermediate state and a two-dimensional mixed state. Since in our case the layer thickness is of the order of the coherence length, it must be concluded that the experimentally observed layer is closer to the TDM state, and regard these experiments as attempts at studying the microscopic structure of the latter.

1. There are several variants[5-8] of the theoretical models of the TDM state of type-I superconductors. Andreev and Dzhikaev[8] have considered a structure consisting of macroscopic superconducting and normal

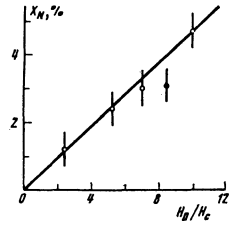

FIG. 15. Concentration X_N of the normal phase, determined from the measurements of the imaginary part of the surface impedance, vs. the supercriticality H_0/H_N at $\theta = 0°$. Sample No. 4. Black circle—value for sample No. 5.

regions. Such a structure is in essence a transition from the intermediate to the TDM state. The thickness of the layer considered in Ref. 8 is much larger than the coherence length, although small compared with the sample dimensions. Layers with thickness on the order of the coherence length were considered in Refs. 5–7.

Andreev and Tekel'[6] pointed out the possible existence, on the sample surface, of a thin ($d \sim \xi$) superconducting layer on whose internal boundary the magnetic field H can assume different values $H \lesssim H_c$. The layer thickness and the order parameter on the sample surface depend on the value of H on the boundary. They neglected the influence of the electric field. Gor'kov and Dorokhov[5] called attention to the fact that the presence of an electric field should make this homogeneous layer unstable. They proposed a model in which the layer is broken up into superconducting strips of macroscopic width separated by narrow ($a_N \sim \xi$) normal regions. The electric field is concentrated in the normal phase and is perpendicular to the phase separation boundary. The flow of current from the normal region into the superconducting region makes the magnetic field on the boundary coordinate-dependent in a direction perpendicular to the strip. The change of the magnetic field leads to a corresponding[6] change in the thickness of the superconducting region and in the order parameter.

Gor'kov and Dorokhov[5] obtained a relation between the parameters of the structure, the average electric field, and the critical magnetic field. In our notation this relation takes the form

$$\frac{4\sigma E_j a_S}{c} \ln \frac{2a_S}{\pi a_N} = H_c, \qquad (1)$$

where σ is the conductivity in the normal state. In the derivation of (1) they assumed a local connection between the current and the electromagnetic field valid at $a_S \gg l_e$, where l_e is the electron mean free path.

The case of extremely strong electric field, when the superconductivity in the layer is almost suppressed and appears only in the form of fluctuations, was considered by Andreev and Bestgen.[7]

The laminar structure of the layer investigated by us is close to the TDM state model proposed by Gor'kov and Dorokhov[5]: the layer thickness is $d \sim \xi_0$, the width of the normal regions is $a_N \sim \xi_0$, and the transverse dimension of the superconducting strips is $a_S \gg a_N$. Substitution of the measured values ($a_S = 2 \times 10^{-2}$ cm, $a_N = 7 \times 10^{-4}$ cm, $E_j = 3 \times 10^{-7}$ V/cm $= 10^{-9}$ cgs esu, and $\sigma = 10^{22}$ cgs esu) yields $H_c = 77$ Oe. The critical field at an experimental temperature $T = 0.4$ K is $H_c = 88$ Oe. The agreement between the calculated and experimental values should be regarded as quite good, in view of the fact that under our conditions the electron mean free path $l_e \sim a_S$.

Notice should be taken of two features of the investigated structure, which distinguish it from the theoretical models: a) the presence of a magnetic field perpendicular to the surface in the normal regions, and b) the dynamic character of the structure. As we shall see below, the second difference is immaterial

for a laminar structure and is of primary significance for the island structure, since the latter can be only dynamic.

2. It follows from our results that the concentration of the normal phase in the investigated structure is determined by the angle between the magnetic field and the surface. A decrease in the inclination angle leads to an increase of the electric field e in the normal regions, since the average electric field E_j is practically independent of θ. The electric field e_0 can take on a value such that the magnetic field of the normal currents reaches a value H_c at a distance of the order of ξ from the surface. In this case one can expect changes in the character of the structure. The corresponding values of the current density $j_0 \sim cH_c/4\pi\xi$ and of the electric field $e_0 = j_0/\sigma$ are reached at a normal-phase concentration

$$X_{N0} \sim 4\pi\sigma E_j \xi / cH_c. \qquad (2)$$

This equation was obtained using the known relation of the macroscopic electrodynamics of the intermediate state $\mathbf{e} = \mathbf{E}/X_N$.[15] Substituting in (2) the experimental values $\sigma = 10^{22}$ cgs esu, $E_j = 10^{-9}$ cgs esu, $\xi = 3\times10^{-4}$ cm, $H_c = 20$ Oe yields at $T = 1.1$ K a value $X_{N0} = 0.06$. It follows from our results (Fig. 14) that this concentration is reached at an approximate inclination angle 0.2°.

Proceeding to the case of a magnetic field $\mathbf{H}_0$ parallel to the surface, we note that besides the already considered TDM state models, a nonstationary layer can exist in principle. The simplest example of such a layer is a homogeneous purely superconducting surface layer that goes over periodically into the normal state. The times during which the layer is in the different states is determined by the damping of the eddy currents and by the value of the magnetic supercooling. It is clear, however, that even an insignificant inhomogeneity of the conditions causes such a layer to become inhomogeneous. If the transition to the normal state does not take place simultaneously over the entire surface, then two normal regions can be produced, in which the magnetic-field component perpendicular to the surface can have opposite signs. This is shown schematically in Fig. 16. The appearance of normal islands in the layer leads to an additional inhomogeneity of the conditions, as a result of which the number of these islands can increase. The motion of the normal regions causes a decrease of the magnetic flux

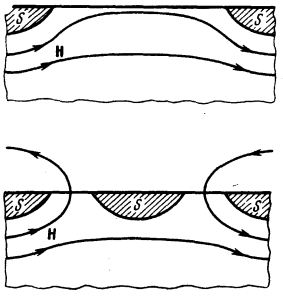

FIG. 16. Schematic representation of the distribution of the magnetic field when a section of the surface goes over into the normal state.

through the sample, and the layer has a resistive character.

The results of experiments in which a magnetic field parallel to the sample surface was turned off point to the presence of precisely such a nonstationary layer. In fact, the concentration of the normal phase and the layer (Fig. 14) is larger than the value expected when account is taken of the real relief of the surface and of the inhomogeneity of the magnetic field. The absence of a correlation between signals of different junctions may be due to the formation and coalescence of regions of the normal phase in the space between the junctions. (Regions in which the magnetic-field components perpendicular to the surface have opposite signs move in opposite directions and can coalesce when they meet.) The asymmetry of the pulse waveform can also be due to formation and coalescence of normal-phase islands.

The velocity of the normal regions in such a nonstationary layer can be estimated. Such an estimate is based on the assumption that the entire change of the magnetic flux in the sample is connected with the motion of the normal islands, and then

$$E_j \sim d\Phi/dt \sim H_c X_N |\mathbf{V}|.$$

Since E_j does not depend on θ, the quantity $X_N|\mathbf{V}|$ should also be conserved. This is actually the case in an inclined magnetic field, since $X_N \sim |\theta|$ (see Fig. 14) and $|\mathbf{V}| \sim 1/|\theta|$.[11] By determining $X_N|\mathbf{V}|$ from measurement at $H_{\perp 0} \neq 0$ and using the measured values of X_N at $H_{\perp 0} = 0$ (Fig. 14), we obtain the corresponding velocity $|\mathbf{V}_0| = 90$ cm/sec. Now, knowing the pulse parameters, we can determine the dimensions of the normal and transition regions produced when a magnetic field parallel to the surface is turned off. At $T = 1.1$ K and $H_0/H_c = 10$ we have

$$a_N \geqslant 2\cdot10^{-3} \text{ cm}, \quad b_N \approx 1\cdot10^{-3} \text{ cm}.$$

3. At the instant of formation of the layer, the voltage on the point junction changes from U_N to U_S. This fact was established by measurements of the absolute value of the voltage. Equality of the heights of the pulses to the voltage jump produced when the layer is formed convinces us that the layer consists of normal and superconducting regions.

The trapezoidal waveform of the pulses is not connected with the junction dimensions, as is confirmed by two results. First, the transition-region dimensions obtained with the aid of junctions of different sizes are equal in value. Second, the dimensions of the transition region for the laminar structure, 3.5×10^{-4} cm $\approx 2.5\xi_0$ at $T = 0.4$ K, differ greatly from the corresponding dimensions for the island structure, 1.8×10^{-3} cm $\approx 5\xi$ at $T = 1.1$ K. We note that transition regions of the same size (from 1×10^{-4} to 5×10^{-4} cm at $T = 0.9$ K) were observed by a microjunction study of the dynamic intermediate state in aluminum.[16] Consequently, the observed pulse waveform is apparently due to the existence, at the boundary between the superconducting and normal regions, of a transition region in which the order parameter varies from zero to the superconducting value. There are grounds for assuming that the signal from the junction is proportional to

the energy gap in the region under the junction. These grounds are the results of measurements of the temperature dependence of the conductivity of N-S point junctions.[1)17]

4. We compare now the dynamics of the laminar structure with the dynamics of the intermediate state, which was considered in detail by Andreev and Sharvin.[20] According to them, the velocity of the phase-separation boundary is

$$V=\frac{c}{H^2X_N}(\mathbf{n}[\mathbf{E}\times\mathbf{H}]), \tag{3}$$

where $\mathbf{H}$ is the magnetic field intensity, $|\mathbf{H}|=H_c$, and $\mathbf{n}$ is a unit vector normal to the phase boundary. The motion is along $\mathbf{n}$.

Under the experimental conditions the direction of the magnetic field in the normal region changes substantially over the thickness of the layer, and on the surface of the sample the field is perpendicular to the layer. The normal regions in the layer move apparently as a unit. It must therefore be assumed that the dynamics of the layer is close to the dynamics of the intermediate state of a current-carrying plate placed in a perpendicular external magnetic field $\mathbf{H}=\mathbf{N}(H_0\cdot\mathbf{N})$. As will be shown below, the results of the calculation made under this assumption explain well the dependence of the magnitude and sign of the velocity on the direction of the magnetic field $\mathbf{H}_0$.

For a plate placed in a perpendicular field $\mathbf{H}_\perp$, neglecting the magnetic field of the transport current, we have[15] $\mathbf{H}=\mathbf{H}_\perp/X_N$ and (3) is transformed into

$$V=c\mathbf{n}[\mathbf{E}\times\mathbf{H}_\perp]/H_\perp^2. \tag{4}$$

In our case the current density in the layer is $\mathbf{j}=\gamma\mathbf{H}_0\times\mathbf{N}$, with $\gamma>0$. For the electric field $\mathbf{E}=X_N\mathbf{e}$ we obtain

$$\mathbf{E}=\frac{\gamma X_N}{\sigma_\perp}\left\{R\sigma_\perp H_c\frac{\mathbf{H}_0\mathbf{N}}{|\mathbf{H}_0\mathbf{N}|}[\mathbf{N}\times[\mathbf{H}_0\times\mathbf{N}]]+[\mathbf{H}_0\times\mathbf{N}]\right\}; \tag{5}$$

here $\sigma_\perp$ is the transverse conductivity in the magnetic field and R is the Hall constant. The electric field in the current direction is

$$E_j=\frac{\gamma X_N}{\sigma_\perp}|[\mathbf{H}_0\times\mathbf{N}]|=\frac{\gamma H_0^2}{\sigma_\perp H_c}|\sin\theta||\cos\theta|. \tag{6}$$

In the experiment with small θ, the value of E_j is practically independent of the angle θ. It follows therefore that $\gamma\sim1/|\sin\theta|\sim1/X_N$, i.e.,

$$\gamma X_N/\sigma_\perp=\lambda=\text{const}. \tag{7}$$

Substituting (5) and (7) in (4) we obtain ultimately

$$V=\frac{c\lambda|\mathbf{H}_0|}{\mathbf{H}_0\mathbf{N}}\left\{R\sigma_\perp H_c\frac{\mathbf{H}_0\mathbf{N}}{|\mathbf{H}_0\mathbf{N}|}\left(\mathbf{n}\left[\frac{\mathbf{H}_0}{|\mathbf{H}_0|}\mathbf{N}\right]\right)-\mathbf{n}\frac{\mathbf{H}_0}{|\mathbf{H}_0|}\right\}. \tag{8}$$

We shall assume hereafter that the orientation of the layers, i.e., $\mathbf{n}$, depends little on the angle between the magnetic field and the surface, and also on the sign of the magnetic field. Under the experimental conditions, the strips are elongated approximately along the projection of $\mathbf{H}_0$ on the surface, therefore the quantity $\mathbf{n}\cdot\mathbf{H}_0/|\mathbf{H}_0|$ changes little when the inclination of the field is changed. Consequently the dependence of the velocity on $\mathbf{H}_\perp$ at constant H_0 takes the form

$$|V|\sim1/|\mathbf{H}_0\mathbf{N}|\sim1/|\mathbf{H}_\perp|,$$

which explains the results of the measurements (see Fig. 9). The meaning of the last relation is simple: when the inclination angle is decreased the electric field in the normal region increases:

$$e=E/X_N\sim1/|H_\perp|.$$

Since the magnetic field in the normal regions is constant and equal to H_c, an increase of e causes a proportional increase of the velocity of the phase-separation boundary.

As seen from (8), the dependence of the sign of the velocity on the direction of $\mathbf{H}_0$ can vary, and two cases are possible. The first is

$$\left|R\sigma_\perp H_c\left(\mathbf{n}\left[\frac{\mathbf{H}_0}{|\mathbf{H}_0|}\times\mathbf{N}\right]\right)\right|>\left|\left(\mathbf{n}\frac{\mathbf{H}_0}{|\mathbf{H}_0|}\right)\right|$$

and the sign of the velocity varies like the sign of the product $(\mathbf{n}\cdot\mathbf{H}_0\times\mathbf{N})$; such a dependence was observed in sample No. 2. The second case occurs when the inverse relation is satisfied and the change of the sign of the velocity coincides with the change of the sign of the expression $(\mathbf{H}_0\cdot\mathbf{n})(\mathbf{H}_0\cdot\mathbf{n})$, in agreement with the results obtained for samples 1 and 3. It should be noted that the laminar structure can become immobile if the strips are so oriented that

$$R\sigma_\perp H_c\left(\mathbf{n}\left[\frac{\mathbf{H}_0}{|\mathbf{H}_0|}\times\mathbf{N}\right]\right)=\mathbf{n}\frac{\mathbf{H}_0}{|\mathbf{H}_0|}.$$

From the experimental results it is easy to estimate the values of the scalar products:

$$\left|\mathbf{n}\frac{\mathbf{H}_0}{|\mathbf{H}_0|}\right|\leqslant0.1,\quad\left|\mathbf{n}\left[\frac{\mathbf{H}_0}{|\mathbf{H}_0|}\times\mathbf{N}\right]\right|\approx1.$$

This corresponds to an approximate orientation of the strips along the projection of $\mathbf{H}_0$ on the surface. For the second case to be possible it is necessary to have $R\sigma_\perp H_c\lesssim0.1$, i.e., the Hall field must be $E_X\lesssim0.1E_j$. This relation is in full agreement with the results of Refs. 21 and 22, where the Hall constant in aluminum was measured and a reversal of its sign was observed. A recalculation of the results of Forsvoll and Holwech[22] as applied to samples with our degree of purity yields a value $H_R=30$ Oe for the magnetic field at which $R(H_R)=0$. The measured velocity $V=1.1$ cm/sec (see Fig. 9) at $H_\perp=1.4$ Oe and $E_j=3\times10^{-7}$ V/cm agrees with the val-

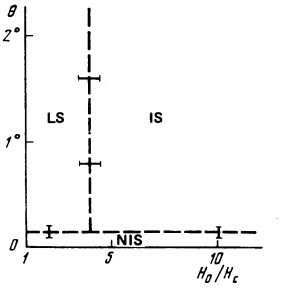

FIG. 17. Regions of existence of different structures under the experimental conditions: *LS*—laminar structure, *IS*—island structure, *NIS*—nonstationary island structure.

ues calculated from Eqs. (6) and (8) if we set the value of the curly bracket in (8) equal to 0.05.

Deviations of the strips from the direction of the projection of H_0 on the surface can be due to several causes. Principal among them are edge effects and pinning. The different action of these factors on different samples apparently causes the first case to occur in sample No. 2 and the second in samples 1 and 3.

The dynamics of the island structure was considered in an earlier study[11] where it was shown that it can be understood on the basis of the laws of the dynamic intermediate state.

CONCLUSION

Experiments in which a magnetic field $H_0 > H_c$ was turned off have shown that the macroscopic properties of the resistive layer produced on the surface of aluminum are close to the properties of the TDM state of type-I superconductors. The microscopic layer consists of moving regions of the normal and superconducting phases, and the magnetic field in the normal regions has a component perpendicular to the layer. The resistive character of the layer is due to energy dissipation in the normal regions, in which the electric field is concentrated. Three types of structure were observed in experiment: stationary laminary, stationary island, and nonstationary island; the regions in which these were observed under our conditions are illustrated in Fig. 17. It is perfectly possible that structures of the same type exist in the TDM layer produced on the inner surface of hollow superconducting cylinders.[1]

The authors are sincerely grateful to V. F. Gantmakher, V. V. Shmidt, and I. L. Landau for helpful discussions.

[1]I. L. Landau and Yu. V. Sharvin, Pis'ma Zh. Eksp. Teor. Fiz. **10**, 192 (1969) [JETP Lett. **10**, 121 (1969)].
[2]I. L. Landau and Yu. V. Sharvin, Pis'ma Zh. Eksp. Teor. Fiz. **15**, 88 (1972) [JETP Lett. **15**, 59 (1972)].
[3]I. L. Landau, Zh. Eksp. Teor. Fiz. **64**, 557 (1973) [Sov. Phys JETP **37**, 285 (1973)].
[4]I. L. Landau, Zh. Eksp. Teor. Fiz. **67**, 250 (1974) [Sov. Phys JETP **40**, 126 (1974)].
[5]L. P. Gor'kov and O. N. Dorokhov, Zh. Eksp. Teor. Fiz. **67**, 1925 (1974) [Sov. Phys. JETP **40**, 956 (1974)].
[6]A. F. Andreev and P. Tekel', Zh. Eksp. Teor. Fiz. **62**, 1540 (1972) [Sov. Phys. JETP **35**, 807 (1972)].
[7]A. F. Andreev and V. Bestgen, Zh. Eksp. Teor. Fiz. **64**, 1865 (1973) [Sov. Phys. JETP **37**, 942 (1973)].
[8]A. F. Andreev and Yu. K. Dzhikaev, Pis'ma Zh. Eksp. Teor. Fiz. **26**, 756 (1977) [JETP Lett. **26**, 590 (1977)].
[9]J. J. Hauser, Phys. Rev. B **10**, 2792 (1974).
[10]V. T. Dolgopolov and S. I. Dorozhkin, Pis'ma Zh. Eksp. Teor. Fiz. **27**, 459 (1978) [JETP Lett. **27**, 420 (1978)].
[11]S. I. Dorozhkin and V. T. Dolgopolov, Solid State Commun. **30**, 205 (1979).
[12]Yu. V. Sharvin, Zh. Eksp. Teor. Fiz. **48**, 984 (1965) [Sov. Phys. JETP **21**, 655 (1965)]
[13]A. Lösche, Kerninduktion, VEB Deutsche Verlag d. Wissenschaftern, Berlin, 1957.
[14]V. T. Dolgopolov and S. S. Murzin, Zh. Eksp. Teor. Fiz. **76**, 1740 (1979) [Sov. Phys. JETP **49**, 885 (1979)].
[15]A. F. Andreev, Zh. Eksp. Teor. Fiz. **51**, 1510 (1966) [Sov Phys. JETP **24**, 1019 (1966)].
[16]M. K. Chien and D. E. Farrell, Phys. Rev B **9**, 2902 (1974).
[17]M. K. Chien and D. E. Farrell, J. Low Temp. Phys. **19**, 75 (1975).
[18]V. N. Gubankov and N. M. Margolin, Pis'ma Eksp. Teor. Fiz. **29**, 733 (1979) [JETP Lett. **29**, 673 (1979)].
[19]S. N. Artemenko, A. F. Volkov, and A. V. Zaitsev, Solid State Commun. **30**, 771 (1979).
[20]A. F. Andreev and Yu. V. Sharvin, Zh. Eksp. Teor. Fiz. **53**, 1499 (1967) [Sov. Phys. JETP **26**, 865 (1967)].
[21]E. S. Borovik, Zh. Eksp. Teor. Fiz. **23**, 83 (1952).
[22]K. Forsvoll and J. Holwech, Philos. Mag. **10**, 921 (1964).

Translated by J. G. Adashko